The effect of acute nicotine on trafficking of AMPA glutamate receptors in rat prefrontal cortex

Chris Baddick

Phil Livingstone, Prof. Wonnacott

Mbiol Year 4

2009-2010

Contents

Table of Figures

Abreviation	Full name
AMPAR	α-amino-3-hydroxy-5-methyl-4-isoxazole-propionic acid type glutamate receptor
ATP	adenosine triphosphate
BS^3	bis-(sulfosuccinimidyl)-suberate
BSA	Bovine serum albumin
CaMKII	calcium and calmodulin dependent
cAMP	cyclic adenosine monophosphate
CPu	caudate putamen
D1R	dopamine d1 like receptor
D2R	dopamine d2 like receptor
D-AP5	D(-)-2-amino-5-phosphonovalcric acid
ERK	extracellular signal regulated kinase
GABA	γ- aminobutyric acid
GluR1	AMPA type 1 subunit
GluR2	AMPA type 2 subunit
GluR3	AMPA type 3 subunit
HP	hippocampus
LTD	long term deppression
LTP	long term potentiation
NAc	nucleus acumbens
nAChR	nicotinic acetylcholine recptor
NMDAR	N-methyl D-aspartic acid type glutamate receptors
MD	maximum density
PFC	prefrontal cortex
PKA	protein kinase A
PKC	protein kinase C
PSD	post synaptic density
SKF	dopamine D1R agonist (6-Chloro-2,3,4,5-tetrahydro-1-phenyl-1H-3-benzazepine hydrobromide)
SNc	substantia nigra pars compacta
ST	striatum
TM	transmembrane
VTA	ventral tegmental area

Table 1 all abbreviations used in the text are listed in alphabetical order.

1. <u>Abstract</u>

Nicotine, the UK's second most commonly used psychostimulant drug, interacts with the nervous system via nicotinic acetylcholine receptors (nAChRs). nAChR modulation of dopaminergic and glutamatergic pathways leads to long and short term changes at synapses. Regulation of AMPA trafficking may be an example of a short term change caused by nicotine. Using bis-(sulfosuccinimidyl)-suberate (BS^3), a membrane impermeable crosslinking reagent, in combination with AMPA subunit specific antibodies and western blotting allowed surface and intracellular populations of AMPA subunits to be distinguished and measured. In response to incubation with 100 µM nicotine for 15 minutes, GluR2 surface expression appeared to increase, whilst GluR1 surface expression appeared to decrease. GluR2 surface expression also increased in response to 10 µM SKF 81297, a dopamine D1R agonist. Phospho-ERK2, a downstream signalling protein which is produced in response to D1R activation, was also probed for. In response to nicotine, production of Phospho-ERK2 increased.

These results suggest that nicotine can alter AMPA subunit trafficking over a short time scale, and this process may be mediated by dopamine release and D1R receptor activation.

This study offers a method in which surface and intracellular populations of AMPARs can be measured. Further

2. <u>Introduction</u>

Nicotine

Twenty one percent of the population of Great Britain are regular users of tobacco (Office for national statistics, 2007), making nicotine the second most commonly used human psychostimulant drug. It is most often administered via tobacco cigarette smoking, and also via smokeless forms such as snuff (Melikian and Hoffmann, 2009). In both cases, many users become drug dependant, and self-administer low level chronic doses over a long time scale. Nicotine interacts with the nervous system via nicotinic acetylcholine receptors (nAChRs). nAChRs are a family of homo- and hetero-pentameric voltage gated cation channels found throughout the central and peripheral nervous systems. nAChR subunits are classified into families based on structural similarity; In mouse brain, α2-7 and β2-4 are known (Gotti et al., 2006). nAChRs have been found on dopaminergic and glutamatergic cell bodies and terminals, and also GABAergic terminals in a wide range of brain regions. The endogenous nAChR ligand acetylcholine, and also nicotine, binds to these receptors and promotes ion influx that may alter firing patterns of a range of neuron subtypes (Albuquerque et al., 2009). Stimulation of nAChRs on dopaminergic cell bodies in the mesencephalon has been shown to both decrease tonic dopamine release and elicit a burst firing response thus increasing the signal to noise ratio (Zhang et al., 2009). nAChRs on glutamatergic terminals are located perisynaptically and act to increase Ca^{2+} levels within the presynaptic terminal. This increase in Ca^{2+} leads to movement of glutamate vesicles to the presynaptic membrane. The prefrontal cortex (PFC) and striatum (ST) are both areas in which nAChRs are known to modulate dopamine and glutamate release.

Nicotine and dopamine in the brain

The ST is a sub-cortical region of the midbrain (See Figure 1). It can be divided into smaller sub-regions according to structure and function; of interest to synaptic plasticity in response to nicotine are the Nucleus acumbens (NAc), part of the ventral ST, and the caudate putamen (CPu), which makes up the dorsal ST. The loss of dopaminergic neurons arising in the SNc and projecting to the ST occurs in Parkinsons' disease (Sandberg and Phillips, 2009), whilst increases in dopamine in the NAc are a known effect of tobacco smoking (Di Chiara, 2002).

The PFC has been implicated in working memory (Uylings et al., 2003, Floresco and Magyar, 2006); the dorsolateral PFC in primates (Goldman-rakic, 1995) and the medial PFC in rodents are structurally similar (Seamans and Yang, 2004) and have high inputs from glutamateric and dopaminergic neurons, which converge onto dendritic spines of deep layer pyramidal neurons . The way in which synapses in this region respond to incoming information may control many aspects of target related behaviour, memory and attention in primates (Williams and Goldman-rakic, 1995). Nicotine improves attention and working memory in both laboratory animals and humans (Mansvelder et al., 2006) and the ability of nicotine to increase dopamine release from ascending dopamine neurons in the PFC offers a mechanism for this (Figure 1).
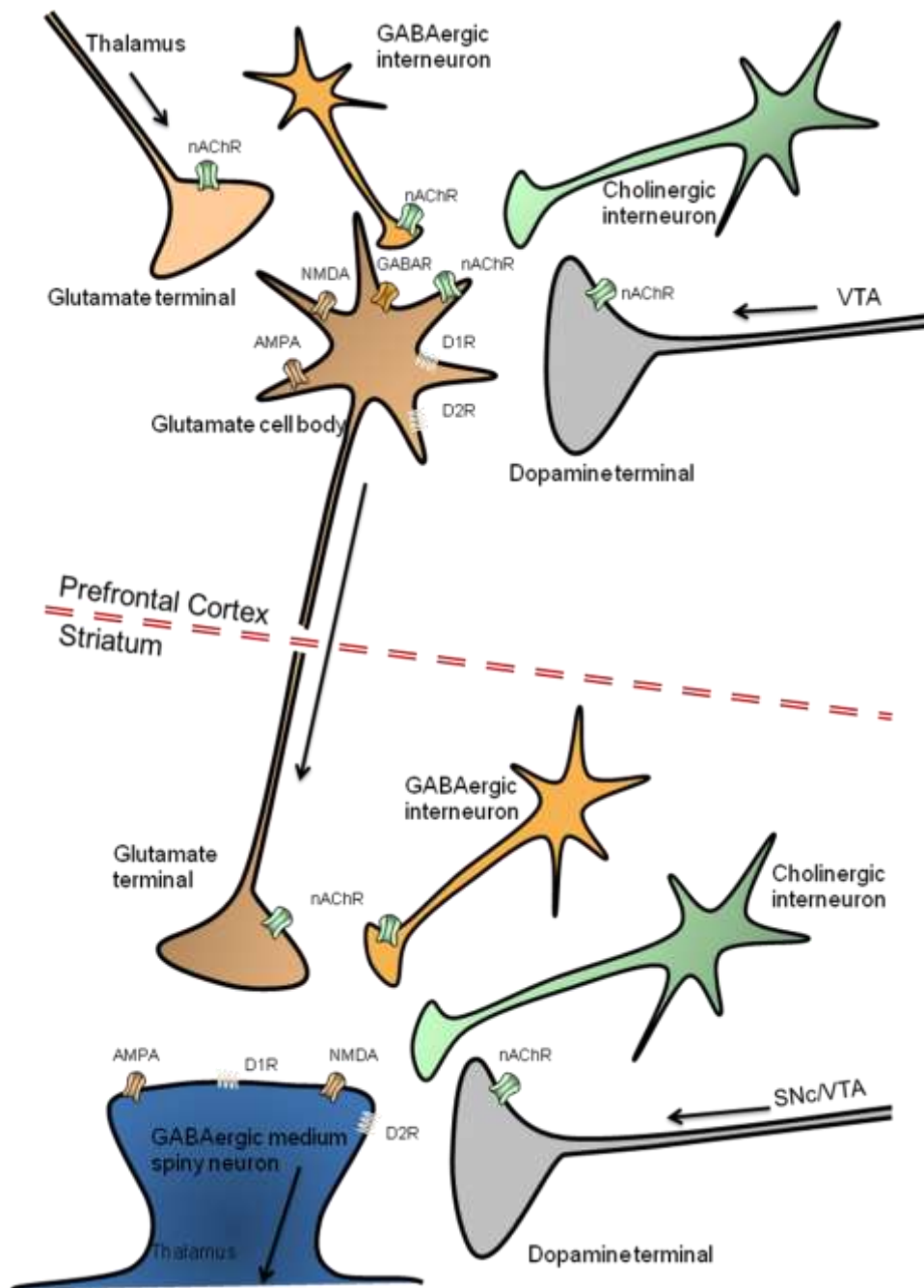
Figure 1 Nicotinic acetylcholine receptors in the prefrontal cortex and striatum. The ascending dopamine pathways are a series of connections originating from the mesencephalon; mainly the Ventral Tegmental Area (VTA) and Substantia Nigra pars compacta (SNc). The terminals of SNc (and a small population of VTA) dopaminergic neurons project to the Caudate Putamen (CPu, dorsal striatum), to form the nigrostriatal pathway. The mesocortical pathway projects from the VTA to the PFC, and the mesolimbic pathway from the VTA to the Nucleus Acumbens (NAc, ventral striatum). nAChR receptors are present on glutamate, dopamine and GABA terminals, and glutamate spines. G-protein coupled dopamine receptors, both D1- like and D2- like are found on glutamate and GABA spines and mediate cAMP controlled enzyme activation, which can lead to changes in AMPA composition, accumulation and function. Through extensive behavioural and biochemical studies, the PFC and ST have been identified as regions stimulated during drug abuse.

AMPA receptors undergo changes during synaptic plasticity

It is a known fact that an increase or decrease in activity at a synapse can cause long and short term plasticity, leading to reinforcement of a pathway (Hayashi et al., 2000). Long Term Potentiation (LTP) (Martinez and Derrick, 1996) and Long Term Depression (LTD) (Artola and Singer, 1993, Linden, 1994) are major forces involved in long lasting synaptic plasticity (Wang et al., 1997) . Various mechanisms for these changes have been discussed and studied in the hippocampus (HP) and in cultured neurons (Malgaroli and Tsien, 1992); one of which is that dopamine release plays a role in altering the composition and expression of post synaptic glutamate receptors (Calabresi et al., 1992). Studies have shown that the induction of LTP and LTD has a substantial effect on the strength of glutamatergic synapses, and these changes are essential for reinforcement of learning and memory (Malenka and Nicoll, 1999). Among the changes seen in glutamatergic neurons during synaptic plasticity are differential membrane trafficking (Ehlers, 2000), post-translational modification (Yang et al., 2009), and modification of individual subtypes within a receptor (Hayashi et al., 2000). These changes have a noticeable effect on function of the receptor. Synaptic scaling, the process where a neuron regulates all of its excitatory synapses to stabilize firing, involves calcium dependant regulation of glutamate receptor trafficking which in turn controls their accumulation (Turrigiano, 2008).

Dopamine release leads to AMPA phosphorylation

Dopamine receptors are seven pass transmembrane G-protein coupled receptors which can be categorised into two main groups which have opposing functions (Neve et al., 2004, Missale et al., 1998) (Figure 2). D1-like receptors (D1R, a group containing D1R and D5R) are activated by higher dopamine concentrations (Surmeier et al., 1995), leading to an activation of phosphorylation enzymes via Gs/olf g-proteins (Greengard et al., 1999). D2-like receptors (D2R, D3R and D4R) activated by low dopamine concentrations causing an inhibition of the

same enzymes via Gi/o g-proteins (Figure 2) (Neve et al., 2004). Gs/olf proteins activate adenyl cyclase which catalyses the formation of cAMP from ATP (Surmeier et al., 1995). cAMP can phosphorylate protein kinase A (PKA), leading to its activation (Greengard et al., 1999). A target of PKA phosphorylation is AMPA type glutamate receptors (those glutamate receptors with α-amino-3-hydroxy-5-methyl-4-isoxazole-propionic acid (AMPA) binding sites) (Keinanen et al., 1990). AMPA receptors (AMPARs) are homo- and heterotetrameric ligand gated ion channels comprising a combination of GluR1-GluR4 subunits (Lu et al., 2009). Each subunit has a weight of approximately 100KDa (Sobolevsky et al., 2009). Like nAChRs, they are members of the cys-loop ligand gated ion channel super family and are the primary receptors involved in the transduction of fast excitatory activity in the mammalian brain (Hansen et al., 2007). The recently published crystal structure of the receptor has confirmed that each subunit has four membrane situated domains; TM1, 3 and 4 are transmembrane, and TM 2 folds 180° inside the membrane to remain on the intracellular side (Sobolevsky et al., 2009). The intracellular C-terminus is the most variable between each subunit, and this is where most protein-protein interactions occur. These interactions have shown to be integral to the regulation of function and organisation of the receptors (Kim and Sheng, 2004, Collingridge et al., 2004, Malinow and Malenka, 2002).
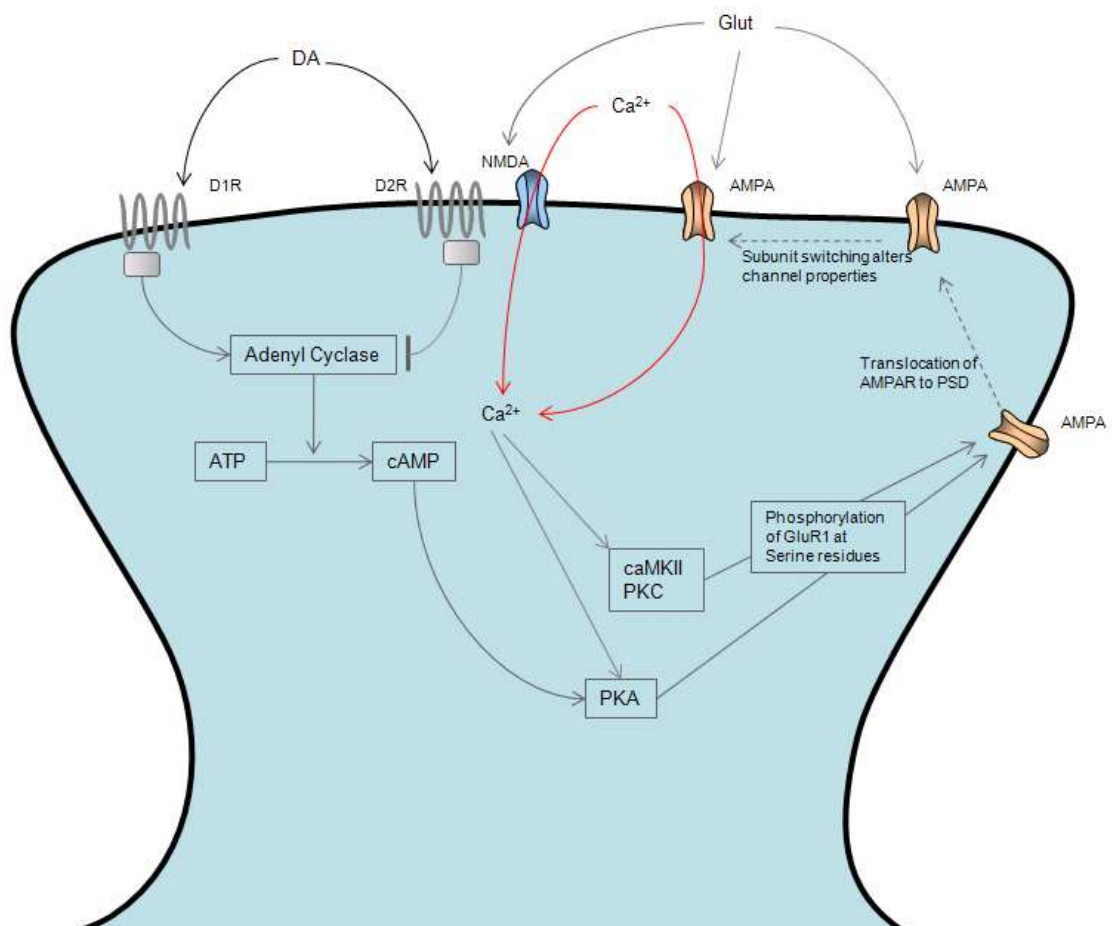
Figure 2 Post synaptic spine of either a deep layer pyramidal glutamate terminal situated in the PFC or a GABAergic medium spiny neuron situated in the Striatum.
D1R activates the enzyme adenyl cyclase which catalyses the formation of cAMP from ATP. cAMP then activates PKA which phosphorylates Ser845 on the C terminus of GluR1 subunits. D2R receptors inhibit adenyl cyclase and cause the opposite effect. D2R receptors are activated by a low concentration of dopamine, whilst D1R receptors require high dopamine levels for activation. Glutamate release can activate NMDA ionotropic receptors leading to an increase in intracellular Ca^{2+}. This increase activates caMKII and PKC which phosphorylate Ser831 and Ser818 of GluR1 respectively, but can also activate Protein phosphatase 2 (calcineurin) which acts to inhibit PKA. Phosphorylation of Serine residues in AMPARs causes a translocation of receptors from a perisynaptic postion into the post synaptic density.

Glutamate release leads to AMPA phosphorylation

Alongside dopamine mediated increase in AMPAR phosphorylation, Ca^{2+} dependant mechanisms also increase phosphorylation and rely on the activity of N-methyl-D-aspartic acid (NMDA) type glutamate receptors (NMDAR) to provide a synaptic activity dependant increase in Ca^{2+} (Ehlers, 2000). nAChRs could therefore induce phosphorylation of AMPARs

via stimulation of either dopamine or glutamate release, in a similar manner observed after cocaine injection (Boudreau and Wolf, 2005). The increase in calcium activates protein kinases including PKA and protein kinase C (PKC), and calcium/calmodulin (CaM) – dependant protein kinase II (CaMKII) (Cammarota et al., 2002). Serine residues in the C-terminus of the GluR1 intracellular loop have been shown to be a target of this regulation; Ser845 is phosphorylated by PKA and Ser818 by PKC (Roche et al., 1996). CaMKII also phosphorylates a PDZ domain in the GluR1 C-terminus (Kim and Sheng, 2004); PDZ domains bind specific sequences in the C-terminus of proteins, which can increase receptor subunit assembly into functional receptors (Hayashi et al., 2000).

AMPA subunit switching

Subunit composition is involved in controlling function and location of AMPARs (Collingridge et al., 2004, Malinow and Malenka, 2002). Under basal conditions, most receptors contain both GluR1 and GluR2; these heteromeric receptors respond to phosphorylation differently than homomeric GluR1 receptors. In hippocampal CA1 pyramidal neurons, CaMKII phosphorylation of Ser831 on GluR1 increases single-channel conductance in homomeric receptors, but not in heteromeric receptors (Oh and Derkach, 2005). This has a large effect on channel function; GluR2 containing receptors have lower channel conductance, lower permeability to Ca^{2+} and Na^+ and decreased opening probability (Swanson et al., 1997, Oh and Derkach, 2005). Recent studies have indicated that synaptic plasticity could be mediated by the recruitment of a class of GluR2 deficient AMPARs to the post-synaptic density, at the same time GluR2 containing receptors are removed from the PSD (Ju et al., 2004). This is supported by studies showing an increase of synaptic strength in response to the inclusion of GluR2 deficient AMPARs at the PSD (Benke et al., 1998, Luthi et al., 2004). These investigations have so far focused on the HP, an area known to undergo LTP. Unlike in the PFC and ST, however, dopamine has marginal involvement in the HP. Further studies will

be needed to determine whether subunit switching is responsible for changes in synaptic strength throughout the brain.

Changes in AMPA expression

The cytoskeleton plays an active role in organisation of the dendritic spines. Spine size and synaptic strength are positively correlated, with larger spines needing more actin microtubules (Collingridge et al., 2004, Malinow and Malenka, 2002). The cytoskeleton must engage in polymerisation in response to synaptic activity. The mean half life of actin filaments in spines is 44 seconds (Star et al., 2002); this shows that the cytoskeleton may play a role in the short term plasticity induced by acute exposure to psycho-stimulants. It is possible that differential interactions between AMPARs and actin microtubules will have an effect on post synaptic trafficking of the receptors (Malinow and Malenka, 2002); mutation of the C-terminus of GluR1 subunits, causing loss of the Ser818 binding site, decreases interaction with the actin associated Protein 4.1N (Shen et al., 2000). Analysis of double-mutant (Ser845Ala/Ser831Ala) mice shows no change in basal level protein trafficking, but do show a decrease in LTP (Lee et al., 2003). This suggests that these regulatory sites are required for later stage trafficking to and from extra synaptic regions of the post synaptic membrane, with or without supplementary NMDAR signalling. Without the increase in Ca^{2+} caused by NMDAR activation, AMPARs are constantly recycled from the post-synaptic membrane to endosomal sorting vesicles, where they are either degraded or reinserted (Park et al., 2004, Ehlers, 2000, Passafaro et al., 2001). It has been shown that reinsertion and endocytosis occurs at an extra synaptic location (Blanpied et al., 2002), and lateral diffusion into the postsynaptic density (PSD, indicated by high levels of the protein PSD-95 in the area) only occurs on activation of NMDARs (Passafaro et al., 2001). The localisation of endocytosis related proteins, such as clathrin, at an extra synaptic site lends further support to this theory (Blanpied et al., 2002). Experiments aiming to simulate LTD conditions have

shown that with a large increase of glutamate, AMPARs will diffuse away from the PSD and be endocytosed at a peripheral location (Ehlers, 2000). This process will lead to an overall decrease in AMPAR numbers in the PSD, thus decreasing signalling. Similarly, blockade of NMDAR signalling by D(-)-2-amino-5-phosphonovalcric acid (D-AP5) does not decrease insertion of AMPARs to extrasynaptic sites, showing this process is NMDAR independent. Also, D-AP5 incubation does not affect dopamine D1 receptor induced colocalization of GluR1 containing receptors near the PSD, showing no requirement for NMDAR stimulation in what has been shown as an early stage of LTP (Gao et al., 2006). Calcium release assays have provided evidence that NMDARs must be stimulated to localise AMPARs to the synaptic area.

The studies described above have made a strong case for ionotropic glutamate receptors being the basis of synaptic change in hippocampal neurons. In regions such as the PFC and ST, which are known to be involved in drug seeking behaviour and addiction, it is unclear how nicotine interacts with these processes. The interactions between nicotine, dopamine signalling and glutamate receptor trafficking are in need of investigation.
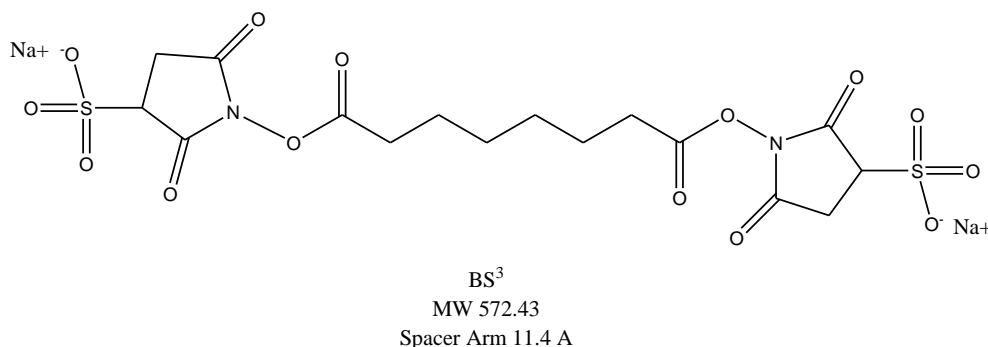
Cross-linking reagent

BS^3
MW 572.43
Spacer Arm 11.4 A

Figure 3 bis(sulfosuccinimidyl)suberate (BS^3) crosslinker molecule was used to bind cell surface proteins, thus creating high molecular weight aggregates.

In order to study the changes in surface expression of AMPARs in isolation from receptors held intracellularly in vesicles, a method was needed to distinguish between each population. The bis-(sulfosuccinimidyl)-suberate (BS^3) crosslinker is a membrane impermeable molecule which binds free primary amino groups (-NH$_2$) of surface expressed proteins to form stable amide bonds. In polypeptides free amino groups are found in lysine (K) residues due to its NH$_2$ side chains. With a spacer length of 11.4 Å, it is able to join two closely situated peptides irreversibly. By binding all surface expressed proteins, a western immunoblotting protocol can be used to probe for each AMPA subunit individually; all surface expressed proteins should appear as a heavier weight band, whilst uncrosslinked intracellular subunits will form a band of ~100kDa. Measuring surface crosslinking in response to nicotine treatments could provide an answer to whether nicotine can directly interact with glutamate receptor trafficking.

Research aims

To develop and optimise a method in which changes in levels of surface expression of AMPAR GluR1 and GluR2 subunits can be measured in response to acute nicotine. To do this, AMPA GluR1-4 specific antibodies will be optimised and used to develop a method in which surface expressed proteins will be bound using BS^3 and measured using western blotting.

Tissue minces will be prepared from rat PFC and ST, and undergo treatment with nicotine and D1R specific agonist SKF81297. Samples will then be treated with BS^3 to bind surface receptors, and western blotting will be used to determine relative surface expression of AMPAR subunits in response to each treatment.

3. <u>Materials and Methods</u>

Materials List

proTEAN® gel electrophoresis and semi dry transfer apparatus from Biorad, Hertfordshire UK. Tris; Glycine; Methanol; Ethanol; Sodium Chloride; Potassium Chloride; calcium chloride dehydrate; potassium dihydrogen phosphate; magnesium sulphate heptahydrate; soudium bicarbonate; from Fisher Scientific, Loughborough UK. BS^3 crosslinking molecule; BCA protein assay kit, from Peirce, Rockford, IL USA. Primary antibodies; Millipore Watford UK. HRP conjugated anti-rabbit and anit-mouse secondary Antibodies; ECL plus and advanced detection systems, nitrocellulose membranes; X-ray film, from GE healthcare, Bucks, UK. Filter paper from Whatman, UK. B-Mercaptoethanol; TEMED, from ICN biochemicals Aurora OH, USA. Blocking Solution from Marvel milk, Dublin, Ireland. Protogel from National Diagnostics, Hull, UK. Parafilm from Pechiney Plastics, Menasha WI, USA. Tween-20, Ammonium monophosphate, D-glucose; Ascorbic acid; Pargyline; Sodium dodecyl sulphate, Nicotine hydrogen tartrate from Sigma, MO USA. Microsoft Excel for windows (2007). Sigmaplot version 8.02a (2004) from Systat software, inc. ImageJ (version 1.42q) free software from NIH, USA (http://rsb.info.nih.gov/ij). GraphPad Prism version 3 from GraphPad Software, Inc. La Jolla CA USA
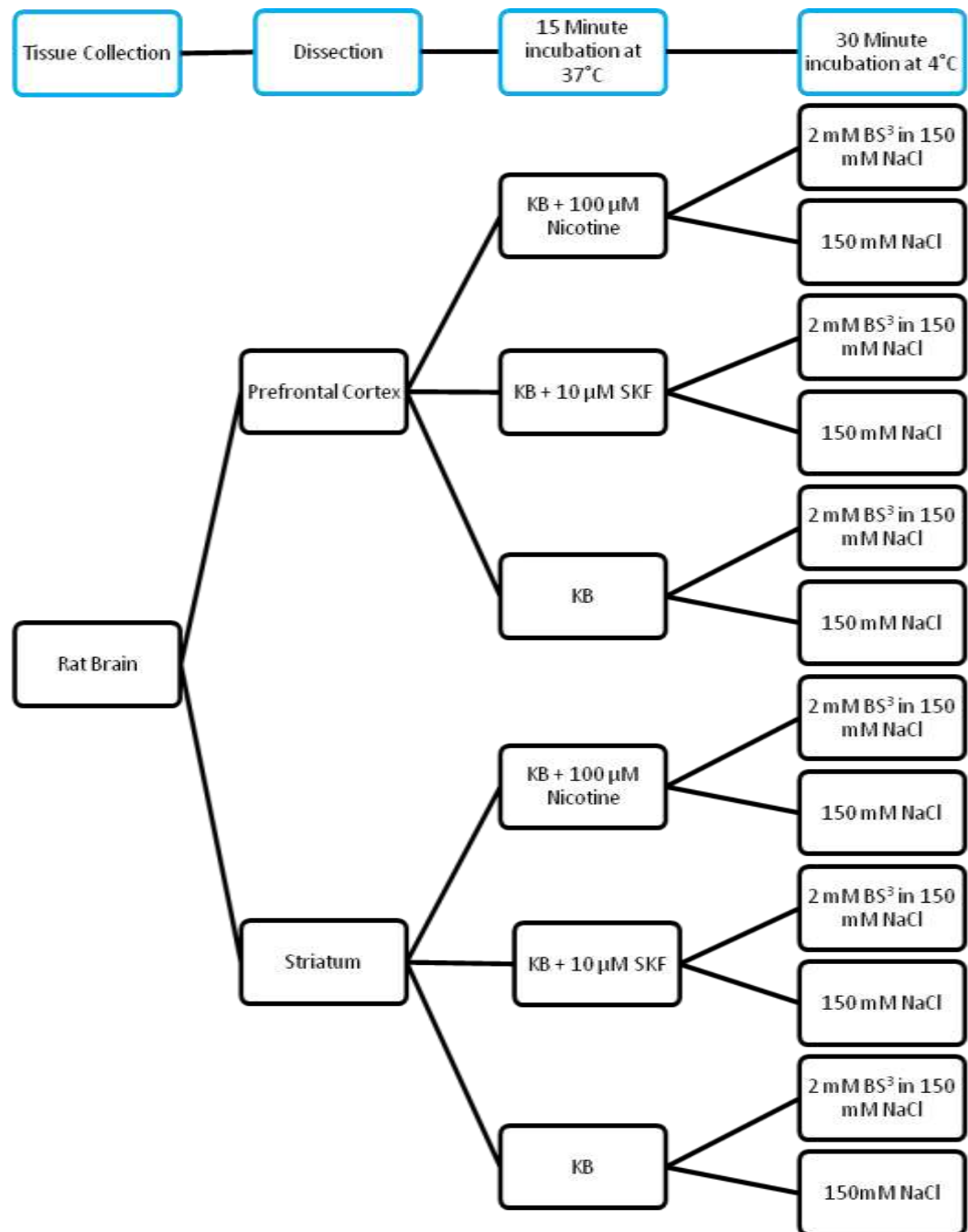
Figure 4 Diagram showing the process of tissue collection and preparation, leading to 12 different experimental conditions. From each animal, the PFC and the Striatum were dissected and chopped using a McIlwain tissue chopper. The tissue was split into 6 conditions to undergo incubation with 100 µM Nicotine in KB, or 10 µM SKF 81297 in KB, or just KB. Each tube was then divided into two; one of which received 2 mM BS[3] crosslinker in 150mM NaCl, or just 150mM NaCl.

Tissue dissection and preparation

Rats (Male Sprague–Dawley rats, 200–300 g supplied by Charles Rivers) were used. Each rat was killed by cervical dislocation then decapitated using a guillotine and brains rapidly removed. Tissue dissections were carried out on a cold dissection platform, and each sample collected was put into ice cold krebs buffer (KB; 118 mM NaCl, 2.4 mM KCl, 2.4 mM CaCl2, 1.2 mM KH2PO4, 1.2 mM MgSO4·7H2O, 25 mM NaHCO3, gassed with oxygen (O_2) for 1 hour at 37 ºC followed by addition of 10 mM d-glucose, 1 mM ascorbic acid. pH 7.4 containing 10 μM pargyline). The ST (including *CPu* and *NAc*) and PFC were dissected. PFC was defined as 3 mm from anterior, 4 mm from bregma and 1 mm from corpus callosum. Tissue was chopped using a McIlwain tissue chopper to give 150 μm prisms; this preparation method allows the retention of a large amount of structural integrity.

The prisms were suspended in KB at 37 ºC and incubated for 7 minutes to allow tissue to settle. KB was then removed and replaced for a further 5 minutes. KB was again removed, and the tissue covered in 1 ml KB and split into 12 micro-centrifuge tubes (Figure 4). Once the tissue had settled in the tubes, KB was removed and replaced with the treatment solutions.

Tissue Treatment

Either 100 μl of 100 μM nicotine (from 10 mM stock in KB at pH 7.4) in KB, or 100 μl 10 μM SKF in KB, or 100 μl KB was added to each tube, and then left at 37 ºC agitating for 15 minutes. After 5 minutes each tube was inverted. Samples were centrifuged for 20 seconds at 13,000 rpm and the supernatant was discarded and the pellet washed twice with 200 μl of ice cold 150 mM NaCl.

BS³ Cross-linking

BS^3 was made to 100 mM in distilled water and then diluted to a working concentration of 2 mM in 150 mM NaCl. 200 μl NaCl or 200 μl NaCl with BS^3 was added to each tube. Incubation was for 30 minutes shaking at 4 ºC; the low temperature reduces internalisation of the crosslinker. To end the reaction tissue was quenched with 1 ml of 100 mM glycine, shaking at 4 ºC for 10 minutes. Another centrifugation for 20 seconds at 13,000rpm allowed removal of the treatment and quenching solutions, before re-suspension in 1% sodium dodecyl sulphate (SDS) .

Western immuno-blotting

Each sample was homogenized by hand in a glass-Teflon tissue homogenizer in 1% SDS in order to preserve the phosphorylation of constituent proteins.   The tissue was then diluted 1:10 with 1 % SDS. The Pierce® BCA protein assay was used to determine the amount of protein per sample. Standards were made by serial dilution of 2mg/ml Bovine Serum Albumin (BSA) stock in 1% SDS. This was used to generate a standard curve of mean absorbance at 572nm. Samples were read in the same plate and GraphPad Prism (version 3.0) software was used to interpolate unknown protein concentrations from the standard curve.

For loading, samples were diluted 3:1 into a 4 x Laemmli buffer (125mM Tris (pH 6.8) 4% SDS, 10% glycerol, 0.02% bromophenol blue) modified by addition of 20% β-mercaptoethanol. The modified 4x Laemmli was then diluted to 1x with 1% SDS and this buffer was used to equalise all protein concentrations,

Western Blotting was undertaken using the Biorad mini Protean™ western blotting apparatus. For separation, a 10% acrylamide gel was used, whilst a 3% gel was used for the stacking phase. Each sample was pipetted into the wells, and the same volume of Pageruler^{TM} prestained protein ladder added to determine approximate band size. The gels

were run for 75 - 130 minutes at 100 V (constant voltage) in SDS-PAGE running buffer (383mM glycine, 50mM Tris, 3.4mM SDS). Preliminary experiments were run for 75 minutes, while cross linking assays were run for 130 minutes in order that heavier weight bands would be separated. After running, gels were soaked for 20 minutes in transfer buffer (48mM Tris, 39mM Glycine, 130mM SDS, 20% v/v Methanol) partly in order to remove the dye front from the gel; primary antibodies have a high affinity for dyes, thus giving erroneous readings. Semi-dry blotting apparatus was used at 20V, 0.45A (constant voltage) for 45 minutes to transfer the protein onto a nitrocellulose membrane. The membranes were blocked for 1 hour at room temperature in blocking solution (5% Marvel milk in TBS buffer with 1% Tween20 (TBS-T)).

Primary antibodies (obtained from Dr. Rob Williams: see acknowledgements) were diluted in 1% blocking solution and incubated at 4°C gentle shaking overnight. These were removed by sequential washes (2 brief rinses, 2 x 5 minutes, and 3 x 15 minutes) in TBS-T. Secondary Antibodies (horseradish peroxidise (HRP) conjugated anti-rabbit or anti-mouse) were also diluted in 1% blocking solution for 2 hours gentle shaking at room temperature, and the same washing process used for removal.

The blots were developed using enhanced chemiluminescence (ECL Plus or Advanced blotting detection systems) for 5 minutes. The reaction relies on the oxidation of luminol to release of light at 428nm. The emitted light allows detection of protein bands, which can be exposed to autoradiograph film for 15 seconds – 20 minutes, depending on band intensity and detection method used.

Band Densitometry

Band densitometry was performed using Image J (version 1.42q). Each blot was scanned into Adobe Photoshop (version CS3) and converted to an 8bit greyscale JPEG image (Figure 5), containing 255 individual grey colours. Each colour in the scale is assigned a number, with 255 being the darkest and 0 being the lightest. Using this method, background density was measured in 3 positions on each blot and the average background subtracted from the density of each band. Bands were measured using a rectangle of 40 pixels wide by 15 pixels tall. The size was calculated by measuring the average band size on each blot. Once densitometry had been performed, all numbers were converted into a percentage using Microsoft excel (2007). All graphs were produced in Sigmaplot version 8.

Figure 5 Each blot was scanned in and saved as an 8 bit greyscale JPEG image. Each image contains 255 shades, which can be measured using ImageJ software. Average intensity of each band was calculated and used to measure relative amounts of protein.

Data analysis

Where possible, conditions were compared using a students' t-test run in Minitab version version 15. Where a significant (at $p < 0.05$) result was found, it is indicated above the bar with * marking the comparison. Statistic comparisons are shown in appendix 3.

4. **Results**

Using AMPA subunit antibodies with frozen striatal tissue

The first experiments were aimed at optimising the western blotting procedure. Antibody concentrations needed to be determined and detection methods refined so that crosslinking assays could be carried out accurately and efficiently. Antibodies specific to particular subunits of AMPA glutamate receptors were used on naïve rat striatal tissue which had been snap frozen using Isopentane prior to preparation of prisms.

Figure 6 Antibody optimization: GluR2 level in Naïve rat striatum. *In vitro* prisms (150 μm) were prepared from snap frozen naïve rat striatum and equalised to a protein concentration of 2 mg/ml. The samples were split into 4 identical replicates and 20 μl (0.04 mg) of each sample was loaded for gel electrophoresis and blots were probed with total GluR2 Ab at 1:500 concentration, followed by 1:1000 HRP conjugated anti-rabbit secondary Ab. No bands were visible in initial experiments.

Figure 6 displays the first experiment carried out using antibodies specific to AMPA glutamate receptor subunits. The first blot used a 1:500 Primary antibody dilution, and a 1:1000 secondary antibody dilution. Each blot was exposed using the ECL Advanced detection system. Extremely high background levels and no indication of bands under any condition meant these blots were unusable, so the experiment was repeated. The negative (white) bands seen in Figure 6 indicate that the high background could have been due to too high a concentration of secondary antibody leading to non-specific binding. Further experiments used a 1:5000 dilution of secondary antibody. Although bands could now be detected, the background was still too high to be useable. A change in detection method from ECL advanced to ECL plus yielded better results.

Actin (Figure 7) was initially chosen as a housekeeping control due to it being an intracellular protein which will not be altered by the test conditions; as described in the introduction, actin undergoes rapid recycling and re-modelling at synapses, but overall expression levels do not change (Star et al., 2002). due to its stability under the experimental conditions, it can be used as a loading control to ensure equal protein concentrations were being loaded into each well. Figure 7 shows a consistent protein density and low background.

Figure 7 Actin level in Naïve rat striatum. . *In vitro* prisms (150 µm) were prepared from snap frozen naïve rat striatum and equalised to a protein concentration of 2 mg/ml. The samples were split into 4 identical replicates and 20 µl (0.04 mg) of each sample was loaded for gel electrophoresis. Each one was probed with total 1:500 actin Ab, followed by 1:5000 HRP conjugated anti-rabbit secondary Ab. Bars represent actin band at 35 kDa.

Optimisation of western blotting

Further optimisation experiments were carried out using the AMPA specific antibodies, with altered concentrations. GluR1, 2, 3 and 4 were probed. The blots which probed for GluR1 and GluR4 did not produce visible bands, even with low background levels. The reason for no bands on the GluR1 blot was unknown but could have been due to the antibody being denatured or otherwise degraded. GluR4 is thought to be restricted to only the Cerebellum, and as such may not have been present in the assayed brain regions. The GluR2 and GluR3 antibodies (Figure 8) produced bands.
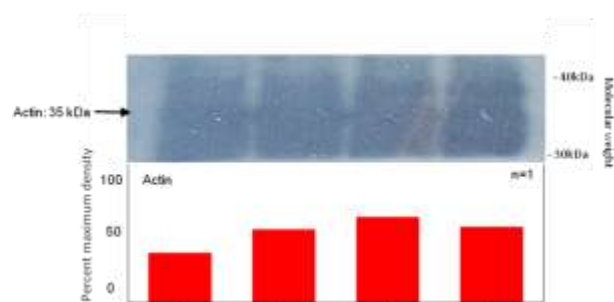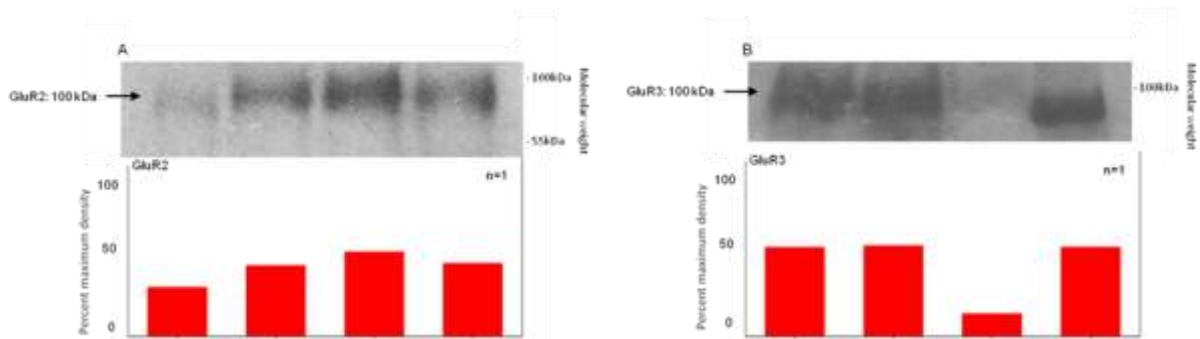

Figure 8   AMPA subunit level in Naïve rat striatum. . *In vitro* prisms (150 μm) were prepared from snap frozen naïve rat striatum and equalised to a protein concentration of 2 mg/ml. The samples were split into 4 identical replicates and 20 μl (0.04 mg) of each sample was loaded for gel electrophoresis. Each one was probed with Total GluR2 (A) or Total GluR3 (B) Ab at 1:500, followed by 1:5000 HRP conjugated anti-rabbit secondary Ab. Bars represent AMPA subunit band at 100 kDa.

The preliminary blots indicated a working concentration of antibodies, and a refined detection method. It was decided to undertake the cross linking assay using the GluR2 antibody. Although the GluR3 antibody had worked, the results were less relevant to our study as GluR3 subunits have not been implicated in changing channel properties in response to subunit switching, as discussed earlier. Due to the unexplained failure of the GluR1 antibody to produce a band, another batch was obtained to be used in further experiments.

In the primary cross-linking assay, prisms were prepared as described in the methods. Nicotine or control solution incubations were followed by a cross linking incubation. The nicotine treated samples were probed for GluR2 at 1:500. The first assay was run for 120 minutes and did not produce bands at the heavier weight position (blot not shown). The band at the 100 kDa position appeared fainter than previous assays, suggesting it may not have contained the entire protein compliment. After 120 minutes of electrophoresis, the 250 kDa band of the protein ladder was at the top of the membrane; to ensure the heavier weight complex had migrated far enough to be transferred onto the membrane, further experiments were run for 130 minutes. The samples used in the first assays had a very low concentration of protein (PFC at 0.2 mg/ml and ST at 0.75 mg/ml), and thus 60 µl of protein, the maximum possible, was loaded into each well to maximise the possibility of measuring a response. In the second crosslinking assay, there was a definite band visible at 250 kDa. However, there were also heavier weight bands visible in non cross linked conditions; this could have been due to samples merging and mixing during loading before the electrophoresis began. Even with ambiguous bands the assay showed that the cross-linking reagent had produced a heavier weight band at approximately 250 kDa. To ensure further experiments were clearer, new tissue was obtained and a further treatment assay performed. The tissue was standardised to 2 mg/ml, thus allowing only 20 µl to be loaded into each well.

Control experiments

Due to the experiments being run for 130 minutes, the 35 kDa actin band had been run off the bottom of the gel. α-tubulin, at 55 kDa, was used as a loading control instead. Figure 9 shows α-tubulin under the same experimental conditions as the crosslinking assays. Each band is at a very similar density, indicating an even amount of protein was loaded into each well; a loading control allows any changes in AMPA subunit level to be interpreted as a response to experimental conditions.

Figure 9 α-Tubulin in response to nicotine and crosslinking in rat PFC and striatum. *In vitro* prisms (150 μm) were prepared from rat PFC (red) or striatum (blue) treated in KB with or without nicotine (100 μM, N) for 15 minutes at 37°C. Treatment was followed by incubation at 4°C for 30 minutes in 150 mM NaCl with or without 2 mM bis(sulfosuccinimidyl)suberate (BS^3) cross-linking reagent (X). Samples were then homogenised by hand using a glass-teflon tissue grinder and equalised to a protein concentration of 2 mg/ml. 20 μl of each sample (0.04 mg of protein) was loaded into wells for electrophoresis for 130 minutes. Samples were probed using total α-Tubulin Ab. Values were calculated from n=2 using pixel densitometry and expressed as a percentage of maximum density. A representitive blot is shown. bars represent α-Tubulin at 55 kDa.

Phospho-ERK1/2 was also used as a control (Figure 10). ERK is an intracellular signalling pathway protein which does not appear on the cell surface, and therefore is unavailable to BS[3]. Additionally, ERK is phosphorylated in response to dopamine signalling and moves to the nucleus to activate gene transcription (Zhai et al., 2008). Using the phospho-ERK1/2 antibody may indicate whether the treatment conditions are leading to downstream signalling changes. Nicotine treated samples trend towards a higher concentration of Phospho-ERK2 at 42 kDa (Figure 10), compared to samples not treated with nicotine. Concentrations of Phospho-Erk1 at 44 kDa do not show any trend of change under any experimental condition.

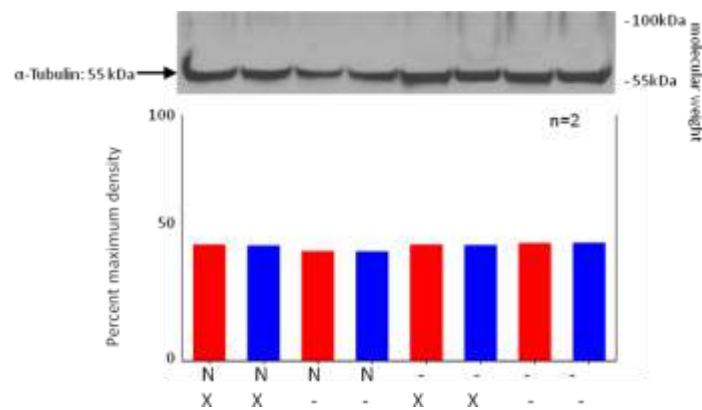**Figure 10 Phospho-ERK 1/2 level in response to nicotine in rat PFC and striatum**. *In vitro* prisms (150 μm) were prepared from rat PFC (red) or striatum (blue) treated in KB with or without nicotine (100 μM, N) for 15 minutes at 37°C. Treatment was followed by incubation at 4°C for 30 minutes in 150 mM NaCl with or without 2 mM bis(sulfosuccinimidyl)suberate (BS[3]) cross-linking reagent (X). Samples were then homogenised by hand using a glass-teflon tissue grinder and equalised to a protein concentration of 2 mg/ml. 20 μl of each sample (0.04 mg of protein) was loaded into wells for electrophoresis for 130 minutes. Samples were probed using Phospho specific ERK 1/2 Ab. Values were calculated from n=2 using pixel densitometry and expressed as a percentage of maximum density. A representitive blot is shown. Upper bars represent Phospho-ERK1 (P-ERK1, 44 kDa). Lower bars represent Phospho-ERK2 (P-ERK2, 42 kDa).

BS³ can be used to determine surface expression of AMPA subunits

A new batch of GluR1 antibody allowed cross-linking to be carried out and tissue probed for GluR1 and GluR2 subunits. Figure 11 shows the surface and intracellular expression of GluR2 in PFC and ST. Intracellular density cannot be directly compared, as in the non cross-linked conditions the intracellular bands is representative on the total population. In crosslinked conditions, it is possible to compare the density of bands in tissue with or without nicotine. The nicotine treated PFC trends towards a higher surface expression of GluR2 (31.5 % of maximum density (MD)) than non nicotine treated PFC (21.5 % MD), whilst no trend can be seen in ST. PFC also appears to be denser than ST in nicotine treated tissue (PFC = 31.5% MD, ST = 17.6% MD), but not in the control conditions (PFC = 21.5% MD, ST = 22.8%MD).
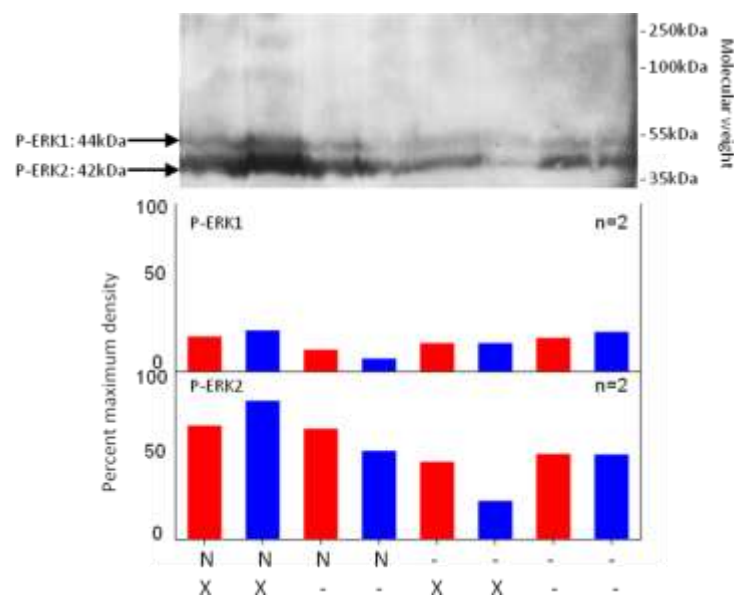

Figure 11 Surface and intracellular expression of GluR2 in response to nicotine in rat PFC and striatum. *In vitro* prisms (150 μm) were prepared from rat PFC (red) or striatum (blue) treated in KB with or without nicotine (100 μM, N) for 15 minutes at 37°C. Treatment was followed by incubation at 4°C for 30 minutes in 150 mM NaCl with or without 2 mM bis(sulfosuccinimidyl)suberate (BS³) cross-linking reagent (X). Samples were then homogenised by hand using a glass-teflon tissue grinder and equalised to a protein concentration of 2 mg/ml. 20 μl of each sample (0.04 mg of protein) was loaded into wells for electrophoresis for 130 minutes. Samples were probed using Total GluR2 Ab. Values were calculated from n=2 using pixel densitometry and expressed as a percentage of maximum density. A representitive blot is shown. Upper bars represent surface GluR2 component (250 kDa). Lower bars represent Intracellular GluR2 component (100 kDa).

The changes in surface expression of GluR1 in response to nicotine (Figure 12) are different to that of GluR2 (Figure 11). Nicotine treated PFC (16 % MD) and ST (15.3 % MD) both appear to have decreased surface expression of GluR1 in comparison to control tissue (PFC = 35.1 % MD, ST = 31.3 % MD). Unlike with GluR2, GluR1 levels are similar in both PFC and ST in tissue with and without nicotine.
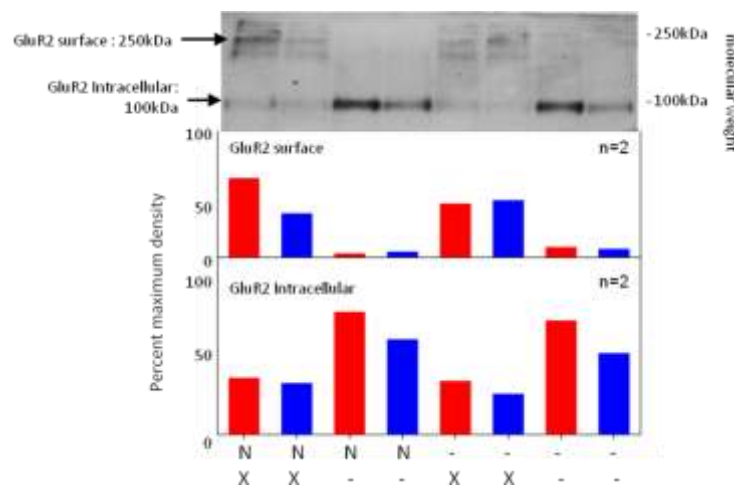

Figure 12 Surface and intracellular expression of GluR1 in response to nicotine in rat PFC and striatum. *In vitro* prisms (150 μm) were prepared from rat PFC (red) or striatum (blue) treated in KB with or without nicotine (100 μM, N) for 15 minutes at 37°C. Treatment was followed by incubation at 4°C for 30 minutes in 150 mM NaCl with or without 2 mM bis(sulfosuccinimidyl)suberate (BS^3) cross-linking reagent (X). Samples were then homogenised by hand using a glass-teflon tissue grinder and equalised to a protein concentration of 2 mg/ml. 20 μl of each sample (0.04 mg of protein) was loaded into wells for electrophoresis for 130 minutes. Samples were probed using Total GluR1 Ab. Values were calculated from n=2 using pixel densitometry and expressed as a percentage of maximum density. A representitive blot is shown. Upper bars represent surface GluR1 component (250 kDa). Lower bars represent Intracellular GluR1 component (100 kDa).

After measuring the total expression of AMPA subunit receptors, the next phase was to measure the phosphorylation states of each subunit in response to the nicotine and cross-linking reagent. The Phospho-GluR1 antibody was used to determine the ratio of phosphorylated subunits at the surface in comparison to intracellularly. The antibody was not obtained until near the end of the project, and only limited quantities were available. For these reasons, optimisation was not possible, and the only assay run with the antibody did not produce useable results. (Figure 13).
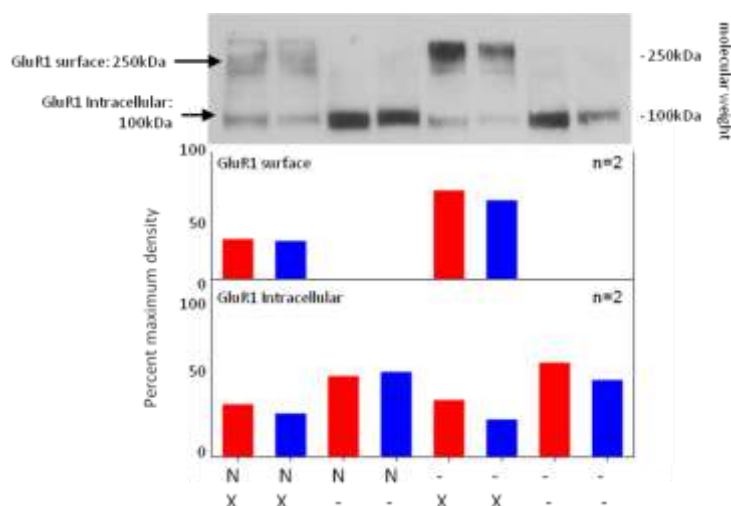

Figure 13 Surface and intracellular expression of Phospho-GluR1 in response to nicotine in rat PFC and striatum. *In vitro* prisms (150 μm) were prepared from rat PFC (red) or striatum (blue) treated in KB with or without nicotine (100 μM, N) for 15 minutes at 37°C. Treatment was followed by incubation at 4°C for 30 minutes in 150 mM NaCl with or without 2 mM bis(sulfosuccinimidyl)suberate (BS^3) cross-linking reagent (X). Samples were then homogenised by hand using a glass-teflon tissue grinder and equalised to a protein concentration of 2 mg/ml. 20 μl of each sample (0.04 mg of protein) was loaded into wells for electrophoresis for 130 minutes. Samples were probed using phospho-GluR1 Ab. Values were calculated from n=2 using pixel densitometry and expressed as a percentage of maximum density. A representitive blot is shown. Upper bars represent surface phospho-GluR1 component (250 kDa). Lower bars represent Intracellular phospho-GluR1 component (100 kDa).

Figure 14 shows tissue probed with GluR2 and α-Tubulin. This tissue was treated with or without 10 μM SKF 81297 for 15 minutes at 37°C. The tissue then underwent cross-linking in the same way as nicotine treated tissue as described above. SKF 81297 (SKF) is a dopamine D1 like receptor agonist. The crosslinked SKF tissue appears to have a higher surface receptor density than crosslinked untreated tissue.
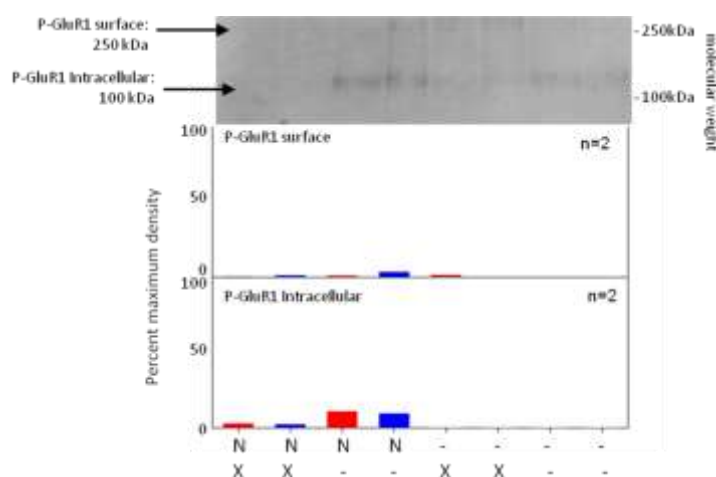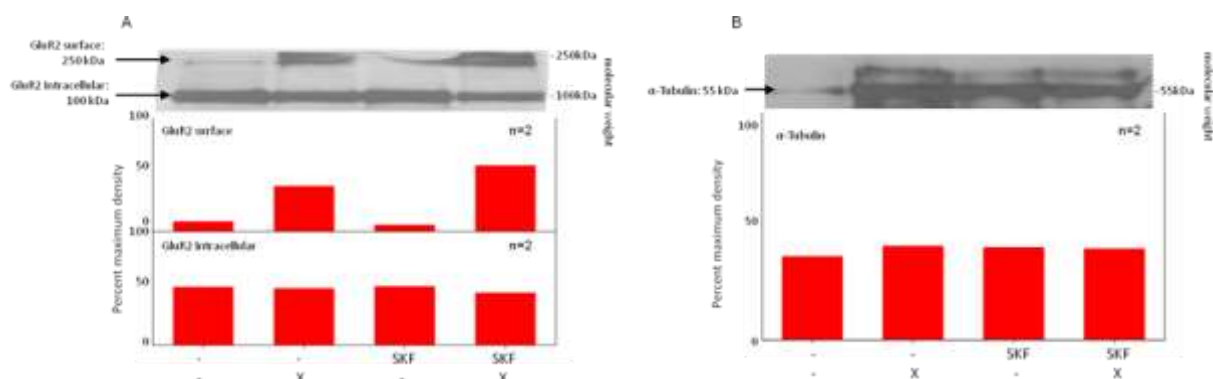
Figure 14 A: Surface and intracellular expression of Total GluR2 in response to SKF 81297 in rat PFC and striatum. *In vitro* prisms (150 μm) were prepared from rat striatum treated in KB with or without SKF 81297 (10 μM, SKF) for 15 minutes at 37°C. Treatment was followed by incubation at 4°C for 30 minutes in 150 mM NaCl with or without 2 mM bis(sulfosuccinimidyl)suberate (BS[3]) cross-linking reagent (X). Samples were then homogenised by hand using a glass-teflon tissue grinder and equalised to a protein concentration of 2 mg/ml. 20 μl of each sample (0.04 mg of protein) was loaded into wells for electrophoresis for 130 minutes. Samples were probed using Total GluR2 Ab. Values were calculated from n=2 using pixel densitometry and expressed as a percentage of maximum density. A representitive blot is shown. Upper bars represent surface GluR2 component (250 kDa). Lower bars represent Intracellular GluR2 component (100 kDa). **B: α-Tubulin in response to SKF 81297 and crosslinking in rat PFC and striatum.** *In vitro* prisms (150 μm) were prepared from rat striatum treated in KB with or without SKF 81297 (10 μM, SKF) for 15 minutes at 37°C. Treatment was followed by incubation at 4°C for 30 minutes in 150 mM NaCl with or without 2 mM bis(sulfosuccinimidyl)suberate (BS[3]) cross-linking reagent (X). Samples were then homogenised by hand using a glass-teflon tissue grinder and equalised to a protein concentration of 2 mg/ml. 20 μl of each sample (0.04 mg of protein) was loaded into wells for electrophoresis for 130 minutes. Samples were probed using total α-Tubulin Ab. Values were calculated from n=2 using pixel densitometry and expressed as a percentage of maximum density. A representitive blot is shown. bars represent α-Tubulin at 55 kDa.

5. <u>Discussion</u>

Development of a cross-linking protocol

This study succeeded in developing and implementing a method in which intracellular and surface expressed populations of AMPA subunits could be distinguished and measured. As described in the introduction, this distinction may be an important step in understanding the short term effects of nicotine on glutamate receptor trafficking.

As each AMPA subunit is thought to have a separate role in the function of assembled receptors, the study relied on using AMPA subunit specific antibodies. Initial experiments were carried out on naïve tissue taken from rat ST. The tissue had been previously frozen before being thawed in order to use in western blotting. Using frozen tissue in conjunction with the AMPA subunit specific antibodies was crucial for further experiments which may require tissue to be frozen for storage before western blotting can be carried out.

Figure 8 represents the first experiment in which bands were produced, however only under two conditions: GluR2 and GluR3. The failure of the GluR1 antibody in this assay meant that experiments proceeded with the GluR2 antibody only. Later experiments used a second batch of GluR1 which had not been tested as extensively.

The cross-linking assay was a novel experiment to the lab group, and the protocol was developed from similar work in other labs. The protocol was based on and developed from previous work by the Wolf research group (Boudreau and Wolf, 2005, Gao and Wolf, 2008). Nicotine was used at a concentration of 100 µM. At this concentration nAChRs are known to be activated, and not desensitized (Marks et al., 1994). SKF 81297 was used at 10 µM based on previous work showing this concentration increased production of cAMP in isolated nerve terminals (Svenningsson et al., 1998). Further experiments would involve a range of time points and treatment concentrations in order to characterise the response of AMPA trafficking to nicotine and SKF 81297 treatment.

Cross-linking assays were carried out for 30 minutes at 4°C. The low temperature was used in order to reduce internalisation of BS³ by crossing the plasma membrane. A range of time points need to be performed in order to determine whether the cross-linking reaction has ended in 30 minutes.

Figure 9 shows the loading control for the cross-linking experiments; standardising each sample to the same protein concentration is essential to ensure that differences in density shown in cross-linking assays are meaningful and not an artefact of error. An equal density also indicates that the same volume of sample was loaded into each well. In some experiments, probing for particular subunits produced no bands on the blot; a loading control shows whether the experiment and protocol have worked; no bands on the blot could be a result in itself, rather than a failure.

Phospho-ERK expression indicates downstream dopamine signalling

Probing for phospho-ERK 1 and phospho-ERK 2 provides two types of data; the fact that ERK is not presented on the cell surface means it should not be available to BS³. Figure 10 shows an example blot of crosslinked and non crosslinked tissue with or without 15 minute nicotine incubation. This tissue was probed with combined Phopho-ERK1/2 antibody; there is no band at a position heavier than 44 kDa which is the weight of Phospho-ERK 1. This study shows that ERK is unavailable to BS³, and therefore that BS³ has not crossed the plasma membrane. This agrees with previous work showing BS³ is unavailable to intracellular proteins (Mattson et al., 1993), and is the ideal compound for measuring surface expression of AMPARs. The second data which can be taken from tissue probed for phospho-ERK is that of downstream dopamine signalling (Zhai et al., 2008). ERK, also known as MAP-Kinase, is phosphorylated in response to activation of Dopamine D1 like receptors, and forms a step in a pathway leading to changes in gene transcription. Figure 10 shows a trend in which

nicotine appears to increase ERK 2 phosphorylation; the mechanism in which this occurs could be via dopamine D1 like receptors.

The effect of nicotine on surface and intracellular expression of GluR1 and GluR2 subunits

Figure 11 and Figure 12 show the effect of nicotine on surface and intracellular expression of AMPA subunits. A limited time frame for experimentation prevented sufficient repetition of each experiment, and therefore all data are combined from n=2. Due to this, no meaningful statistical tests can be used to determine significant differences between conditions. In Figure 11, however, there is a trend towards nicotine treated crosslinked PFC samples having a higher surface expression than non nicotine treated samples; this could suggest that 100 μM nicotine incubated with the prisms for 15 minutes increases trafficking of AMPA GluR2 subunits to the cell surface. Conversely, Figure 12 indicates nicotine could decrease GluR1 surface expression in PFC and ST. The intracellular component of both GluR1 and GluR2 does not appear to be altered in response to nicotine; this fact coupled with an increase in surface expression suggests that receptors being added to the surface population may be newly synthesised, or in the case of reduced expression, that receptors are being removed from the surface and degraded in the lysosome.

By combining data from PFC and ST tissue, an n=4 can be used to test significance. No significant difference (p=0.280) can be seen in surface expression of AMPA GluR2 subunits between crosslinked tissue treated with or without nicotine. Under the same conditions, nicotine treated tissue had a significantly lower (p=0.002) surface expression of AMPA GluR1 subunits (mean = 16.94 ± 0.81 SEM) than non nicotine treated crosslinked tissue (mean = 32.10 ± 1.0 SEM)

These results suggest that nicotine could have a role on the AMPA subunit trafficking.

The effect of SKF 81297 on surface and intracellular expression of GluR1 and GluR2 subunits

The cross-linking assays in which tissue was treated with the dopamine D1R agonist SKF 81297 represents the first in a number of experiments needed to answer how nicotine may cause AMPA trafficking. As described in Figure 2, dopamine offers a mechanism in which activation of D1Rs could lead to phosphorylation of serine residues in AMPA subunits, thus leading to characteristic changes in expression and trafficking. Figure 14 shows that tissue treated with SKF has a marginally higher surface expression of GluR2 than untreated crosslinked tissue. This correlates with the trends shown in nicotine treated tissue. This result indicates that an increase in activation of D1Rs could be responsible for the effect of nicotine on AMPA trafficking. To determine whether dopamine receptor activation is entirely responsible for the effect of nicotine on trafficking, a number of pharmacological assays would need to be carried out. If blockade of dopamine receptors prevented the nicotine induced change in trafficking it could be determined that dopamine is the mediator of these changes. To compound this, dopamine re-uptake could be blocked to measure whether the response increases. Blockade of glutamate and GABA receptors should also be carried out in order to determine these pathways are not involved.

The effect of acute nicotine on trafficking of AMPA glutamate receptors in rat prefrontal cortex

Successful development of a protocol to measure the effect of nicotine on AMPA surface expression is an important step in understanding the role of nicotine in short term synaptic changes. In combination with pharmacological blockade and potentiation of pathway components, the method could also be used to determine the mechanisms in which receptors move to and from the membrane.

6. **References**

Office for national statistics, 2007; General Household survey 2007, see http://www.statistics.gov.uk/cci/nugget.asp?id=313 (accessed 09/12/09)

ALBUQUERQUE, E. X., PEREIRA, E. F. R., ALKONDON, M. & ROGERS, S. W. 2009. Mammalian Nicotinic Acetylcholine Receptors: From Structure to Function. *Physiological Reviews,* 89**,** 73-120.

ARTOLA, A. & SINGER, W. 1993. LONG-TERM DEPRESSION OF EXCITATORY SYNAPTIC TRANSMISSION AND ITS RELATIONSHIP TO LONG-TERM POTENTIATION. *Trends in Neurosciences,* 16**,** 480-487.

BENKE, T. A., LUTHI, A., ISAAC, J. T. R. & COLLINGRIDGE, G. L. 1998. Modulation of AMPA receptor unitary conductance by synaptic activity. *Nature,* 393**,** 793-797.

BLANPIED, T. A., SCOTT, D. B. & EHLERS, M. D. 2002. Dynamics and regulation of clathrin coats at specialized endocytic zones of dendrites and spines. *Neuron,* 36**,** 435-449.

BOUDREAU, A. C. & WOLF, M. E. 2005. Behavioral sensitization to cocaine is associated with increased AMPA receptor surface expression in the nucleus Accumbens. *Journal of Neuroscience,* 25**,** 9144-9151.

CALABRESI, P., MAJ, R., PISANI, A., MERCURI, N. B. & BERNARDI, G. 1992. LONG-TERM SYNAPTIC DEPRESSION IN THE STRIATUM - PHYSIOLOGICAL AND PHARMACOLOGICAL CHARACTERIZATION. *Journal of Neuroscience,* 12**,** 4224-4233.

CAMMAROTA, M., BEVILAQUA, L. R. M., VIOLA, H., KERR, D. S., REICHMANN, B., TEIXEIRA, V., BULLA, M., IZQUIERDO, I. & MEDINA, J. H. 2002. Participation of CaMKII in neuronal plasticity and memory formation. *Cellular and Molecular Neurobiology,* 22**,** 259-267.

COLLINGRIDGE, G. L., ISAAC, J. T. R. & WANG, Y. T. 2004. Receptor trafficking and synaptic plasticity. *Nature Reviews Neuroscience,* 5**,** 952-962.

DI CHIARA, G. 2002. Nucleus accumbens shell and core dopamine: differential role in behavior and addiction. *Behavioural Brain Research,* 137**,** 75-114.

EHLERS, M. D. 2000. Reinsertion or degradation of AMPA receptors determined by activity-dependent endocytic sorting. *Neuron,* 28**,** 511-525.

FLORESCO, S. B. & MAGYAR, O. 2006. Mesocortical dopamine modulation of executive functions: beyond working memory. *Psychopharmacology,* 188**,** 567-585.

GAO, C., SUN, X. & WOLF, M. E. 2006. Activation of D1 dopamine receptors increases surface expression of AMPA receptors and facilitates their synaptic incorporation in cultured hippocampal neurons. *Journal of Neurochemistry,* 98**,** 1664-1677.

GAO, C. & WOLF, M. E. 2008. Dopamine receptors regulate NMDA receptor surface expression in prefrontal cortex neurons. *Journal of Neurochemistry,* 106**,** 2489-2501.

GOLDMAN-RAKIC, P. S. 1995. CELLULAR BASIS OF WORKING-MEMORY. *Neuron,* 14**,** 477-485.

GOTTI, C., ZOLI, M. & CLEMENTI, F. 2006. Brain nicotinic acetylcholine receptors: native subtypes and their relevance. *Trends in Pharmacological Sciences,* 27**,** 482-491.

GREENGARD, P., ALLEN, P. B. & NAIRN, A. C. 1999. Beyond the dopamine receptor: the DARPP-32/Protein phosphatase-1 cascade. *Neuron,* 23**,** 435-447.

HANSEN, K. B., YUAN, H. J. & TRAYNELIS, S. F. 2007. Structural aspects of AMPA receptor activation, desensitization and deactivation. *Current Opinion in Neurobiology,* 17**,** 281-288.

HAYASHI, Y., SHI, S. H., ESTEBAN, J. A., PICCINI, A., PONCER, J. C. & MALINOW, R. 2000. Driving AMPA receptors into synapses by LTP and CaMKII: Requirement for GluR1 and PDZ domain interaction. *Science,* 287**,** 2262-2267.

JU, W., MORISHITA, W., TSUI, J., GAIETTA, G., DEERINCK, T. J., ADAMS, S. R., GARNER, C. C., TSIEN, R. Y., ELLISMAN, M. H. & MALENKA, R. C. 2004. Activity-dependent regulation of dendritic synthesis and trafficking of AMPA receptors. *Nature Neuroscience,* 7**,** 244-253.

KEINANEN, K., WISDEN, W., SOMMER, B., WERNER, P., HERB, A., VERDOORN, T. A., SAKMANN, B. & SEEBURG, P. H. 1990. A FAMILY OF AMPA-SELECTIVE GLUTAMATE RECEPTORS. *Science,* 249**,** 556-560.

KIM, E. J. & SHENG, M. 2004. PDZ domain proteins of synapses. *Nature Reviews Neuroscience,* 5**,** 771-781.

LEE, H. K., TAKAMIYA, K., HAN, J. S., MAN, H. Y., KIM, C. H., RUMBAUGH, G., YU, S., DING, L., HE, C., PETRALIA, R. S., WENTHOLD, R. J., GALLAGHER, M. & HUGANIR, R. L. 2003. Phosphorylation of the AMPA receptor GluR1 subunit is required for synaptic plasticity and retention of spatial memory. *Cell,* 112**,** 631-643.

LINDEN, D. J. 1994. LONG-TERM SYNAPTIC DEPRESSION IN THE MAMMALIAN BRAIN. *Neuron,* 12**,** 457-472.

LU, W., SHI, Y., JACKSON, A. C., BJORGAN, K., DURING, M. J., SPRENGEL, R., SEEBURG, P. H. & NICOLL, R. A. 2009. Subunit Composition of Synaptic AMPA Receptors Revealed by a Single-Cell Genetic Approach. *Neuron,* 62**,** 254-268.

LUTHI, A., WIKSTROM, M. A., PALMER, M. J., MATTHEWS, P., BENKE, T. A., ISAAC, J. T. R. & COLLINGRIDGE, G. L. 2004. Bi-directional modulation of AMPA receptor unitary conductance by synaptic activity. *Bmc Neuroscience,* 5.

MALENKA, R. C. & NICOLL, R. A. 1999. Neuroscience - Long-term potentiation - A decade of progress? *Science,* 285**,** 1870-1874.

MALGAROLI, A. & TSIEN, R. W. 1992. GLUTAMATE-INDUCED LONG-TERM POTENTIATION OF THE FREQUENCY OF MINIATURE SYNAPTIC CURRENTS IN CULTURED HIPPOCAMPAL-NEURONS. *Nature,* 357**,** 134-139.

MALINOW, R. & MALENKA, R. C. 2002. AMPA receptor trafficking and synaptic plasticity. *Annual Review of Neuroscience,* 25**,** 103-126.

MANSVELDER, H. D., VAN AERDE, K. I., COUEY, J. J. & BRUSSAARD, A. B. 2006. Nicotinic modulation of neuronal networks: from receptors to cognition. *Psychopharmacology,* 184**,** 292-305.

MARKS, M. J., GRADY, S. R., YANG, J. M., LIPPIELLO, P. M. & COLLINS, A. C. 1994. DESENSITIZATION OF NICOTINE-STIMULATED RB-86(+) EFFLUX FROM MOUSE-BRAIN SYNAPTOSOMES. *Journal of Neurochemistry,* 63**,** 2125-2135.

MARTINEZ, J. L. & DERRICK, B. E. 1996. Long-term potentiation and learning. *Annual Review of Psychology,* 47**,** 173-203.

MATTSON, G., CONKLIN, E., DESAI, S., NIELANDER, G., SAVAGE, M. D. & MORGENSEN, S. 1993. A PRACTICAL APPROACH TO CROSS-LINKING. *Molecular Biology Reports,* 17**,** 167-183.

MELIKIAN, A. A. & HOFFMANN, D. 2009. Smokeless tobacco: a gateway to smoking or a way away from smoking. *Biomarkers,* 14**,** 85-89.

MISSALE, C., NASH, S. R., ROBINSON, S. W., JABER, M. & CARON, M. G. 1998. Dopamine receptors: From structure to function. *Physiological Reviews,* 78**,** 189-225.

NEVE, K. A., SEAMANS, J. K. & TRANTHAM-DAVIDSON, H. 2004. Dopamine receptor signaling. *Journal of Receptors and Signal Transduction,* 24**,** 165-205.

OH, M. C. & DERKACH, V. A. 2005. Dominant role of the GluR2 subunit in regulation of AMPA receptors by CaMKII. *Nature Neuroscience,* 8**,** 853-854.

PARK, M., PENICK, E. C., EDWARDS, J. G., KAUER, J. A. & EHLERS, M. D. 2004. Recycling endosomes supply AMPA receptors for LTP. *Science,* 305**,** 1972-1975.

PASSAFARO, M., PIECH, V. & SHENG, M. 2001. Subunit-specific temporal and spatial patterns of AMPA receptor exocytosis in hippocampal neurons. *Nature Neuroscience,* 4**,** 917-926.

ROCHE, K. W., OBRIEN, R. J., MAMMEN, A. L., BERNHARDT, J. & HUGANIR, R. L. 1996. Characterization of multiple phosphorylation sites on the AMPA receptor GluR1 subunit. *Neuron,* 16**,** 1179-1188.

SANDBERG, S. G. & PHILLIPS, P. E. M. 2009. *Phasic Dopaminergic Signaling: Implications for Parkinson's Disease*, Humana Press Inc.

SEAMANS, J. K. & YANG, C. R. 2004. The principal features and mechanisms of dopamine modulation in the prefrontal cortex. *Progress in Neurobiology,* 74**,** 1-57.

SHEN, L., LIANG, F., WALENSKY, L. D. & HUGANIR, R. L. 2000. Regulation of AMPA receptor GluR1 subunit surface expression by a 4.1N-linked actin cytoskeletal association. *Journal of Neuroscience,* 20**,** 7932-7940.

SOBOLEVSKY, A. I., ROSCONI, M. P. & GOUAUX, E. 2009. X-ray structure, symmetry and mechanism of an AMPA-subtype glutamate receptor. *Nature,* 462**,** 745-745.

STAR, E. N., KWIATKOWSKI, D. J. & MURTHY, V. N. 2002. Rapid turnover of actin in dendritic spines and its regulation by activity. *Nature Neuroscience,* 5**,** 239-246.

SURMEIER, D. J., BARGAS, J., HEMMINGS, H. C., NAIRN, A. C. & GREENGARD, P. 1995. MODULATION OF CALCIUM CURRENTS BY A D-1 DOPAMINERGIC PROTEIN-KINASE PHOSPHATASE CASCADE IN RAT NEOSTRIATAL NEURONS. *Neuron,* 14**,** 385-397.

SVENNINGSSON, P., LINDSKOG, M., ROGNONI, F., FREDHOLM, B. B., GREENGARD, P. & FISONE, G. 1998. Activation of adenosine A(2A) and dopamine D-1 receptors stimulates cyclic AMP dependent phosphorylation of DARPP-32 in distinct populations of striatal projection neurons. *Neuroscience,* 84**,** 223-228.

SWANSON, G. T., KAMBOJ, S. K. & CULLCANDY, S. G. 1997. Single-channel properties of recombinant AMPA receptors depend on RNA editing, splice variation, and subunit composition. *Journal of Neuroscience,* 17**,** 58-69.

TURRIGIANO, G. G. 2008. The Self-Tuning Neuron: Synaptic Scaling of Excitatory Synapses. *Cell,* 135**,** 422-435.

UYLINGS, H. B. M., GROENEWEGEN, H. J. & KOLB, B. 2003. Do rats have a prefrontal cortex? *Behavioural Brain Research,* 146**,** 3-17.

WANG, J. H., KO, G. Y. P. & KELLY, P. T. 1997. Cellular and molecular bases of memory: Synaptic and neuronal plasticity. *Journal of Clinical Neurophysiology,* 14**,** 264-293.

WILLIAMS, G. V. & GOLDMAN-RAKIC, P. S. 1995. MODULATION OF MEMORY FIELDS BY DOPAMINE D1 RECEPTORS IN PREFRONTAL CORTEX. *Nature,* 376**,** 572-575.

YANG, G., XIONG, W., KOJIC, L. & CYNADER, M. S. 2009. Subunit-selective palmitoylation regulates the intracellular trafficking of AMPA receptor. *European Journal of Neuroscience,* 30**,** 35-46.

ZHAI, H. F., LI, Y. Q., WANG, X. & LU, L. 2008. Drug-induced alterations in the extracellular signal-regulated kinase (ERK) signalling pathway: Implications for reinforcement and reinstatement. *Cellular and Molecular Neurobiology,* 28**,** 157-172.

ZHANG, T., ZHANG, L., LIANG, Y., SIAPAS, A. G., ZHOU, F. M. & DANI, J. A. 2009. Dopamine Signaling Differences in the Nucleus Accumbens and Dorsal Striatum Exploited by Nicotine. *Journal of Neuroscience,* 29**,** 4035-4043.

7. <u>Acknowledgements</u>

Professor Sue Wonnacott – Supervisor

Phil Livingstone – Post-graduate advisor

Dr. Rob Williams – Provision of Antibodies

8. Appendices

Appendix 1: Buffer and chemical solution formulas

Buffer	Chemical	Volume	Buffer	Chemical	Volume
TBS-T	Tris	2.42 g	**Krebs Buffer**	NaCl	3.45 g
	NaCl	8.0 g		KCl	0.09 g
	d.H2O	800 ml		CaCl2 2H2O	0.18 g
	pH to 7.6 with HCl			KH2PO4	0.08 g
	d.H2O	200		MgSO4.7H2O	0.15 g
	Tween-20	1 ml		NaHCO3	1.05 g
				Gas at 37°C for 1 hour	
SDS-Page	Glycine	72 g		D-Glucose	0.9 g
	Tris	15 g		Ascorbic Acid	0.09 g
	10% SDS	25 ml		Pargyline	62 µl of 80 mM stock
	d.H2O	475 ml			
			4x Laemmli Buffer	Tris	3 g
Transfer Buffer	Tris	2.91 g		Glycerol	40 ml
	Glycine	1.465 g		10% SDS	2.5 ml
	10% SDS	1.875 ml		Bromophenol Blue	5 mg
	methanol	100 ml			
	d.H2O	398.125 ml		d.H20	60 ml
	pH	9			
			Resolving Gel (10%)	Tris	2.5 ml
Stacking Gel	Tris	975 µl		30% Protogel	3.4 ml
	30% Protogel	660 µl		dH2O	4.1 ml
	d.H2O	2.2 ml		10% SDS	100 µl
	10% AMPS	20 µl		10% AMPS	50 µl
	TEMED	4 µl		TEMED	5 µl

Appendix 2: Densitometry data

All data is expressed as a percentage of maximum density, as described in the Materials and Methods section.

Column	Figure 7 Actin	Figure 8 A GluR2	Figure 8 B GluR3	Figure 9 α-tubulin
1	31.8098	33.0737	60.1035	70.9863
2	46.7576	47.798	61.2965	70.518
3	54.7502	57.1035	15.3651	66.9784
4	48.4953	49.3949	60.2494	66.9024
5				70.9925
6				70.7729
7				71.9729
8				72.0165

Column	Figure 10 P-ERK 2	P-ERK 1	Figure 11 GluR2 Intracellular	GluR2 Surface
1	47.8231	14.8698	22.7075	31.5184
2	58.082	17.4538	20.5957	17.5639
3	46.4682	9.4451	48.7357	1.7725
4	37.3278	5.6882	37.9337	2.4737
5	32.7741	12.178	21.478	21.4533
6	16.418	12.2235	16.4514	22.7773
7	36.0898	14.3246	45.338	4.3247
8	35.7875	16.779	32.369	3.5596

Column	Figure 12 GluR1 Intracellular	GluR1 Surface	Figure 13 P-GluR1 Intracellular	P-GluR1 Surface
1	20.9149	16.0278	2.031	0.5757
2	17.3016	15.2627	1.6427	1.0306
3	32.0412	1.5433	6.8694	0.8651
4	33.6843	0.5822	5.9729	2.4447
5	22.5725	35.1016	0.2627	0.9086
6	15.0125	31.2573	0.4086	0.7729
7	37.3525	0.06	0.0227	0
8	30.5412	0.4667	0.7149	0

Column	Figure 14 A GluR2 intracellular	GluR2 surface	Figure 14 B α-tubulin
1	51.4898	9.0886	55.0106
2	50.3612	40.2451	61.8655
3	52.0831	6.1294	61.08
4	46.531	58.3753	60.2024

Appendix 3: Students T-test on combined data from PFC and ST to show trends of nicotine on surface expression of AMPA glutamate receptors.

A	B	C	D		E	F	G	H
GluR2	GluR2	GluR2	GluR2		GluR1	GluR1	GluR1	GluR1
N	N	-	-		N	N	-	-
X	-	X	-		X	-	X	-
31.5184	1.7725	21.4533	4.3247		16.0278	1.5433	35.1016	0.9176
17.5639	2.4737	22.7773	3.5596		15.2627	0.5822	31.2573	1.0083
21.9236	0.2345	17.2356	1.2416		17.5502	0.0285	33.059	0.06
28.3052	1.0349	20.234	2.0006		15.9012	1.6382	34.9834	0.4667

Table 2 Densitometry data expressed as a percentage of maximum density. Data for each condition are combined from PFC (n=2) and ST (n=2) to give total n=4.

No significant difference (p = 0.280) between nicotine treated crosslinked tissue (mean = 24.83 ± 3.1 SEM) vs. Non nicotine treated crosslinked tissue (mean = 20.43 ± 1.2 SEM) probed for AMPA GluR2 subunit.

```
Two-sample T for A vs C

    N    Mean   StDev   SE Mean
A   4   26.33    6.06      3.0
C   4   20.43    2.37      1.2


Difference = mu (A) - mu (C)
Estimate for difference:  5.90
95% CI for difference:  (-4.45, 16.26)
T-Test of difference = 0 (vs not =): T-Value = 1.81  P-Value = 0.167  DF = 3
```

Significant difference (p = 0.002) between nicotine treated crosslinked tissue (mean = 16.94 ± 0.81 SEM) vs. Non nicotine treated crosslinked tissue (mean = 32.10 ± 1.0 SEM) probed for AMPA GluR1 subunit.

```
Two-sample T for E vs G

    N    Mean   StDev   SE Mean
E   4   16.94    1.62      0.81
G   4   32.10    2.00       1.0


Difference = mu (E) - mu (G)
Estimate for difference:  -15.16
95% CI for difference:  (-18.48, -11.85)
T-Test of difference = 0 (vs not =): T-Value = -11.77  P-Value = 0.002  DF =
5
```